

Conclusions: Among middle-aged individuals, significantly higher T2 relaxation time values were observed for the incidence cohort compared to those from the control cohort at baseline and after 36 months in the weight-bearing medial femur compartment. T2 values increased in the incidence and control group from baseline to 36 month follow-up, but differences in changes were non significant. Highest T2 value increases were found in the medial compartments, suggesting pronounced cartilage degeneration in the medial compared to the lateral joint compartments.

426

CORRELATIONS BETWEEN HIP STRUCTURE ANALYSIS AND ACTIVE SHAPE MODELLING IN SUBJECTS WITH OSTEOARTHRITIS

R.J. Barr¹, J.S. Gregory¹, K. Yoshida¹, S. Alesci², R.M. Aspden¹, D.M. Reid¹
¹Univ. of Aberdeen, Aberdeen, United Kingdom; ²Pfizer, Collegeville, PA

Purpose: We have used Active Shape Modelling (ASM) to describe the outline of the hip joint through the coordinates of landmark points. ASM of the hip allows sensitive quantification of variation in hip shapes characteristic of OA by using a small number of independent variables (modes of variation). Others have investigated the potential of femoral morphometry as an imaging biomarker for osteoarthritis. In addition to bone mineral density measurements the latest generation of dual energy x-ray absorptiometry scanners incorporate Advanced Hip Analysis (AHA), providing an opportunity to compare ASM and Hip Structural Analysis (HSA) output. The aim of this study was to assess correlations between hip shape assessed by ASM and HSA measures in OA subjects with diverse disease severity.

Methods: Subjects were recruited using the local Radiology Information System. 62 subjects, that encompassed the full spectrum of OA KLG, identified as having had a pelvic radiograph in the last 12 months, were invited to undergo a DXA scan of both femurs using an iDXA scanner (GE Medical Systems). AHA data consisting of 8 HSA measures; cross-sectional moment of inertia (CSMI), cross sectional area of the neck (CSA), distance from the centre of mass to the superior neck (y), distance from head centre to section of minimum CSMI along neck axis (d1), distance from head centre to neck/shaft axis intersection (d2), average neck diameter (d3), shaft angle (alpha) and neck/shaft angle (theta) and hip axis length (HAL) were automatically calculated for each subject. Using DXA images, each hip was assigned KLG. An 85 point ASM was applied to each image that included the proximal femur, osteophytes, and parts of the pelvis to provide a comprehensive model of the hip joint. Outputs from the ASM are independent "Modes of Variation" that describe changes in the shape of the hip. Spearman Correlations were used to assess the association between the first 5 modes of ASM variation, KLG and AHA measures.

Results: Correlation coefficients and P-values for Spearman correlation analysis for the first 5 modes of variation, AHA measures and KLG are shown in Table.

Table 1. Correlation between AHA measures, KLG and the first 5 modes of variation (sig. highlighted in bold)

	HAL	CSMI	CSA	d1	d2	d3	y	alpha	theta	KLG
KLG	0.31	0.51	0.40	0.17	-0.25	0.55	0.55	-0.09	-0.11	-
	0.017	<0.001	0.002	0.19	0.053	<0.001	<0.001	0.500	0.42	
Mode1	0.28	0.46	0.28	-0.03	0.21	0.44	0.41	-0.06	-0.36	0.10
	0.028	<0.001	0.03	0.84	0.098	<0.001	0.001	0.65	0.004	0.45
Mode2	-0.33	0.02	-0.02	-0.35	-0.70	0.06	0.39	-0.04	0.25	-0.05
	0.01	0.90	0.86	0.006	<0.001	0.649	0.002	0.41	0.049	0.72
Mode3	0.32	0.32	0.32	0.36	0.07	0.41	0.43	0.06	0.39	0.25
	0.013	0.012	0.012	0.004	0.61	0.001	0.001	0.65	0.002	0.049
Mode4	0.05	0.39	0.44	0.20	-0.19	0.27	0.38	-0.04	-0.13	0.45
	0.69	0.002	<0.001	0.17	0.14	0.034	0.003	0.79	0.32	<0.001
Mode5	-0.13	0.26	0.18	0.18	-0.16	0.23	0.09	0.24	-0.40	0.10
	0.33	0.043	0.16	0.18	0.23	0.075	0.48	0.065	0.001	0.45

Conclusions: These results demonstrate that variation in shape captured by ASM is moderately associated with some, but not all, of the measures of hip morphometry captured by AHA. Further discriminatory power to detect early OA or those who may go on to require total hip replacement may be gained by combination of these measures.

427

COMPOSITIONAL ULTRASTRUCTURE OF THE NUCLEUS PULPOSUS AT 1.5T MRI: A COMPARATIVE STUDY OF T2 AND T2* MAPPING TECHNIQUES

A. Dudek¹, F.W. Roemer^{2,1}, G. Welsch³, M. Wimmer⁴, S. Trattnig³, K. Bohndorf¹
¹Klinikum Augsburg, Augsburg, Germany; ²Boston Univ. Sch. of Med., Boston, MA; ³Univ. of Vienna, Vienna, Austria; ⁴Technical Univ. Munich, Munich, Germany

Purpose: The compositional integrity of the annulus fibrosus and the nucleus pulposus are paramount for the biomechanical function of the intervertebral disk. MRI-based T2 mapping techniques provide important information on the interaction of water molecules and the collagen network. In addition, T2* relaxation time mapping may provide additional biochemical information of the intervertebral disk's ultrastructure, which seems to correlate with standard quantitative T2 mapping, but with the additional benefit of three-dimensional acquisition capability. Aim of study was to compare T2 with T2* relaxation times of normal intervertebral disks of the lumbar spine using T2 and T2* maps applying two different definitions (circular- and rhomboid-shaped) regions of interest (ROI).

Methods: Lumbar MRI was performed on 10 volunteers without lumbar pain (Oswestry Score 0) on a 1.5 T system (Magnetom Avanto, Siemens, Erlangen, Germany). 30 disks of the L2/3 to the L5/S1 levels were assessed. The protocol for MR measurements consisted of a multi-echo spin-echo sequence and a gradient-echo sequence for the T2* mapping. Parameters for T2 mapping were: TR 1,200 ms, 11 echoes of 12.7 ms increments. T2* maps were constructed with a TR of 102 ms and echo times of 4.76ms increments. Number of averages was 16 for T2* maps and 2 for T2 maps. Field of view for both acquisitions was 280x280 mm, slice thickness of 8mm, bandwidth 120Hz/pixel for T2 maps and 200Hz/pixel for T2* maps. Total combined acquisition time for both sequences was 17 min 43 sec. T2 and T2* relaxation times were obtained using a pixel wise, monoexponential, non-negative least squares (NNLS) fit analysis. Circular- and rhomboid-shaped regions of interest (ROI) were drawn manually by two readers separately using OsiriX version 3.6.1 as DICOM-viewer. The rhomboid-shaped ROI was defined as a rhomboid between the median line of the sagittal and the cranio-caudal margins of the disc. The circular-shaped ROI was defined as a circle in the center of the nucleus pulposus with the center in the median line of the sagittal margins (Figure 1). Mean T2 and T2* values and standard deviation were calculated. For correlations between T2 and T2* values Pearson's coefficients were calculated using PASW statistics version 17.0.2 for mac (SPSS Institute, Chicago, IL, USA).

Results: Mean age of volunteers was 26.3 years (range 22-32 years), mean BMI was 21.3 (range 18.4-24.4). Both definitions of ROI showed a significant correlation of the T2* and T2 values. The coefficients between T2 and T2* maps for the circular ROI was 0.56 (p<0.001) and for the rhomboid ROI 0.55 (p = 0.002). Mean T2* values were 52.9ms ± 19.1ms (range 9-82ms); mean T2 values were 128.4ms ± 29.1 ms (range 68-187ms) using the ROI circle. The mean T2* values were 45.9ms ± 16.8ms (range 9-69ms) and mean T2 values for the rhomboid were 110.7 ms ± 24.4 ms (range 58-159ms).

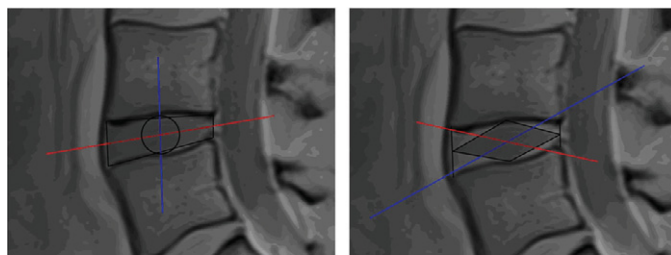


Figure 1. Definition of region of interest (ROI) for T2 and T2* mapping. Image on the left shows example of circular ROI. Image on the right depicts rhomboid ROI. Parts of the annulus fibrosus will be included using rhomboid ROI.

Conclusions: T2* and T2 values correlate moderately for both of the defined ROIs. Lower T2 and T2* values for the ROI "rhomboid" were observed due to larger parts of the annulus fibrosus being included in the ROI analysis. Generally T2* showed lower relaxation times with a higher standard deviation than T2. The presented results implicate that T2* and T2 assess the intervertebral disc ultrastructure differently.